Nanocapsules Embedded in Natural Rubber Latex Gloves

Saovaree Tanpantree,[1] Pakorn Opaprakasit,[2] Surapich Loykulnant,[3] Wiyong Kangwansupamonkon,[4] Pramuan Tangboriboonrat[1]

[1]*Department of Chemistry, Faculty of Science, Mahidol University, Phyathai 10400, Bangkok, Thailand*
[2]*School of Bio-Chemical Engineering and Technology, Sirindhorn International Institute of Technology, Thammasat University, Pathumthani 12120, Thailand*
[3]*National Metal and Materials Technology Center, National Science and Technology Development Agency, Pathumthani 12120, Thailand*
[4]*National Nanotechnology Center, National Science and Technology Development Agency, Pathumthani 12120, Thailand*

Received 27 October 2009; accepted 22 January 2010
DOI 10.1002/app.32132
Published online 29 March 2010 in Wiley InterScience (www.interscience.wiley.com).

ABSTRACT: To prepare medical gloves containing disinfectant agent, poly(methyl acrylate) (PMA) with $\overline{M}_w$ of 550 K was synthesized via the iniferter technique and then used for encapsulating disinfectant agent, i.e., chlorhexidine digluconate (CHD), droplets. The CHD-PMA nanocapsules suspended in a sodium dodecyl sulfate aqueous solution having 93% encapsulation efficiency were successfully embedded between the outermost and inner layers of γ-radiation vulcanized natural rubber (RVNR) latex films by the coagulant dipping process. A RVNR/CHD-PMA nanocapsules/RVNR three-layer structure was revealed by the contact angle measurement, ATR-FTIR and SEM. Both the tensile strength and elongation at break of the three-layer film were also measured. © 2010 Wiley Periodicals, Inc. J Appl Polym Sci 117: 1798–1803, 2010

Key words: elastomers; films; morphology; rubber; surfaces

INTRODUCTION

Natural rubber (NR) latex has been widely used for the production of gloves for medical personnel. Although NR has good mechanical properties which are unmatched by most synthetic rubbers, the gloves, especially those used by surgeons and dentists, are frequently perforated or torn during employment due to needles or sharp objects.[1,2] Medical gloves containing disinfectant droplets were, therefore, developed.[3,4] When the glove is punctured, the antiseptic agent would neutralize infectious agents carried by the needle and a significant reduction of infection rate is obtained.[5]

It is worth mentioning that gloves made of synthetic rubber are rather thick when compared with gloves made of NR latex, hence, tactile sensation and manual dexterity are decreased. The preparation of NR gloves containing chlorhexidine digluconate (CHD), possessing activity against Gram-positive and Gram-negative bacteria, in the form of nanocapsules has been studied.[6–8] Recently, precipitation of poly(methyl acrylate) (PMA) with weight average molecular weight ($\overline{M}_w$) of 470 K onto nanodroplets of a CHD aqueous solution has been applied to prepare nanocapsules by changing the gradient of dichloromethane/cyclohexane.[8] The CHD-PMA capsules were then redispersed in 2% w/v sodium dodecyl sulfate (SDS) aqueous solution before depositing onto the surface of γ-radiation vulcanized natural rubber (RVNR) latex sheet.

In this work, we report the preparation of a three-layer thin film where the outermost and inner layers were RVNR and the active middle layer containing CHD-PMA nanocapsules (RVNR/CHD-PMA nanocapsules/RVNR) by using the coagulant dipping process. To obtain the capsule's wall which is strong enough to prevent any premature release, yet delicate enough to break up under the required circumstances, the synthesis of PMA with $\overline{M}_w$ of 550 K was attempted. The thermal iniferter technique based on controlled radical polymerization under mild conditions was selected for the PMA synthesis.[9] Increases in encapsulation efficiency and capsule's size which would allow the effective release of the disinfectant agent for neutralization of infectious agents were aimed for. The water contact angle measurement,

Correspondence to: P. Tangboriboonrat (scptb@mahidol.ac.th).

Contract grant sponsor: The Thailand Research Fund/Commission on Higher Education; contract grant number: RTA5180003.

Contract grant sponsors: Thailand Graduate Institute of Science and Technology, National Science and Technology Development Agency.

attenuated total reflection-Fourier transform infrared spectroscopy (ATR-FTIR), and scanning electron microscopy (SEM) were used for characterization of the coated surfaces. The effects of coagulant ($Ca(NO_3)_2$) concentration on the thickness, tensile strength, and elongation at break of the RVNR/CHD-PMA nanocapsules/RVNR three-layer film were also investigated.

EXPERIMENTAL

Materials

Methyl acrylate (MA) monomer (Fluka, Purum) was purified by passing through a column packed with neutral and basic aluminum oxide (Fluka, Purum) and the iniferter, i.e., *N*-bromosuccinimide (Aldrich, >98%) was recrystallized and dried under vacuum before use. Other reagents, i.e., dichloromethane (Lab-scan, AR), cyclohexane (Lab-scan, AR), methanol (Lab-scan, AR), deuterated chloroform (Wimad), tetrahydrofuran (THF) (Lab-scan, AR), soybean phosphatidylcholine or lecithin (MP Biochemicals), sodium dodecyl sulfate (Fluka, GC), 20% w/v CHD (Sigma), calcium nitrate ($Ca(NO_3)_2$) (TSL chemicals, AR), and Teric 16A16 (East Asiatic, AR) were used as received. The commercial RVNR latex was kindly supplied by the Siam Okamoto Co. (Pathumthani, Thailand).

Synthesis of PMA

Polymerization of PMA using the thermal iniferter was carried out according to the method previously reported.[10] The PMA were synthesized by mixing *N*-bromosuccinimide ($0.68 \times 10^{-2}M$) with MA monomer (11.11*M*) for 300 min. The $\overline{M}_w$ of the PMA was determined by gel permeation chromatography (Waters, 150-CV) at 30°C using THF as eluent. For the chemical structure and end group analysis, PMA (10 mg) dissolved in $CDCl_3$ (2 mL) was analyzed by proton-nuclear magnetic resonance spectroscopy (^{1}H-NMR) (Bruker, DP×400).

Preparation of CHD-PMA nanocapsules

The CHD-PMA nanocapsules, stabilized by lecithin (100 mg), in cyclohexane were prepared by using the controlled nanoprecipitation technique described elsewhere.[6,8] 0.5% w/v SDS aqueous solution (10 mL) was then added into cyclohexane (10 mL) containing the nanocapsules. After evaporation of the cyclohexane by using a rotary evaporator (Buchi, Rotavapor R200) at 40°C for 15 min, the capsules suspended in SDS aqueous solution were obtained.

The sizes of the CHD nanodroplets and CHD-PMA nanocapsules were measured with a dynamic light scattering apparatus (Malvern, Zetasizer NanoZS). The charge density of the nanocapsules redispersed in SDS aqueous solution was determined by a microelectrophoresis apparatus (Malvern, Zetasizer nanoZS). The morphology of the CHD-PMA nanocapsules was examined by Transmission Electron Microscopy (TEM) (JEOL, JEM-2010). The encapsulation efficiency was determined by using ^{1}H-NMR, where deuterated water and a known amount of pyrazine were applied as an external solvent and a calibration product, respectively.[6] The mass of CHD in a nanocapsule was calculated from the area ratio of peaks at 7.66 to 9.07 ppm corresponding to aromatic-protons of CHD and pyrazine, respectively.

Preparation of RVNR/CHD-PMA nanocapsules/RVNR three-layer films

The three-layer film of RVNR/CHD-PMA nanocapsules/RVNR was prepared by the coagulant dipping process. A glass mold was first immersed for 5 s in various concentrations of $Ca(NO_3)_2$ coagulant solution (5, 10, and 15% w/v) mixed with nonionic wetting agent (0.1% w/v Teric 16A16). Thereafter, the mold was dipped in 45% total solid content of RVNR latex. The middle layer containing disinfectant agent was produced by dipping the partially dry first layer in 5% w/v $Ca(NO_3)_2$ for 5 s and, subsequently, in 1% CHD-PMA nanocapsules redispersed in SDS aqueous solution for various dipping times. The sample was washed with Milli-Q water via a series of three rinsing baths and dried at room temperature before being analyzed by water contact angle measurement (G-1, Kruss). Each value of the contact angle reported is the average of at least 10 separate drops of water on a given surface. ATR-FTIR spectra of the samples were recorded on a Bruker EQUINOX 55 spectrometer (32 scans at 4 cm^{-1} resolution) by employing a Ge ATR crystal with face angle of 45° in a single-reflection mode.

The outermost layer was subsequently prepared by following the same procedure as that used in the first step. Finally, the three-layer thin film was dried in an oven at 65°C for 15 min. The surface morphology of RVNR inner and outer layers and that of CHD-PMA nanocapsules deposited onto the rubber film was examined by SEM (Hitachi, S-2500).

The thickness of the three-layer film was measured with a digital caliper (KEIBA) at 10 different areas of each sample. The dumbbell specimens were used for tensile testing (Instron, model 5566), stamped out of the three-layer film by using a sharp die according to DIN 53504. For each sample, at least five specimens were tested with a crosshead speed of 100 mm/min using a load cell of 1000*N*.

RESULTS AND DISCUSSION

Characterization of CHD-PMA nanocapsules

The synthesized PMA having $\overline{M}_w$ of 550 K and molecular weight distribution ($\overline{M}_w/\overline{M}_n$) of 1.6 was used for the preparation of capsule's shell. The size of monodisperse CHD droplet was 251 ± 7 nm, whereas that of the nanocapsules suspended in cyclohexane and in SDS aqueous solution were 385 ± 7 and 386 ± 18 nm, respectively. The zeta potential value of the CHD-PMA nanocapsules in SDS aqueous solution which was constant at about −95 mV, confirmed the electrostatic stabilization of the capsules in the medium. From the similar size of CHD-PMA nanocapsules in both media, it can be deduced that a tight molecular interlocking of the long PMA chains effectively entrapped the CHD. The result was confirmed by the high-encapsulation efficiency of CHD-PMA nanocapsules dispersed in cyclohexane (100%) and those redispersed in SDS aqueous solution (93%), as determined by ^{1}H-NMR. A well-defined structure of nanocapsules redispersed in 0.5% SDS aqueous solution, observed under TEM, is shown in Figure 1.

Characterization of CHD-PMA nanocapsules deposited onto RVNR latex film

Water contact angles of the CHD-PMA nanocapsules deposited onto the RVNR latex film are plotted in Figure 2 versus dipping times.

The results show that the water contact angle of the RVNR surface covered with CHD-PMA nanocapsules abruptly decreased from 95° to 46° within the first 3 min of dipping time. After immersing for 3 min, the contact angle approached a constant value, which implies complete coverage of the CHD-PMA nanocapsules on the rubber surface. The low water contact angle confirms the presence of CHD-PMA nanocapsules, whose surface beared lecithin and/or SDS molecules. The present results agree with the values of water contact angle of poly(ether urethane) grafted with lecithin and the gelatin particles stabilized by SDS which were 43° and 50°, respectively.[11,12]

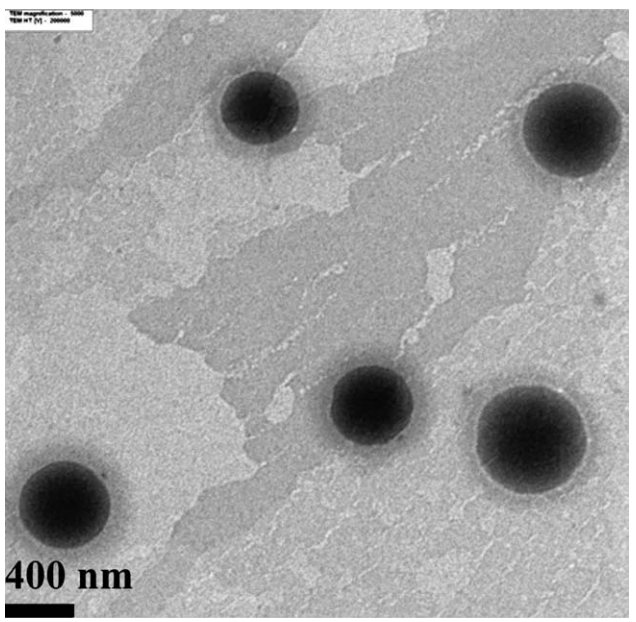

Figure 1 TEM micrograph of CHD-PMA nanocapsules redispersed in 0.5% of SDS aqueous solution.

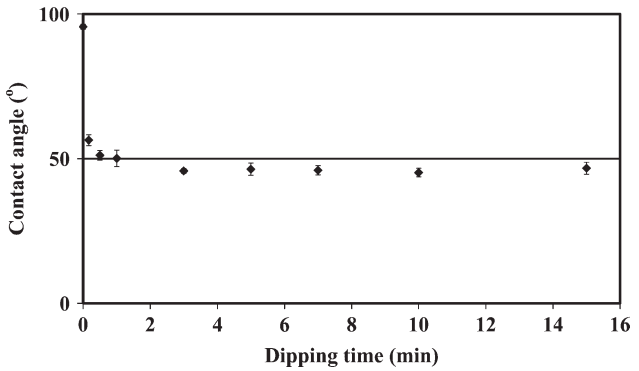

Figure 2 Water contact angles of RVNR film coated with CHD-PMA nanocapsules as a function of dipping time.

The ATR-FTIR spectra of RVNR and CHD-PMA coated-RVNR films are shown in Figure 3 as a function of dipping time.

In the spectrum of RVNR, characteristic peaks at 2961, 2922, 2856 (C—H stretching), 1450, 1378 (C—H bending of —CH_3) and 837 cm^{-1} (C—H deformation of *cis* C=C—H) are seen. In addition, a weak C=O stretching band is observed at 1725 cm^{-1} due to a trace amount of carbonyl groups generated during vulcanization.[13] After deposition of PMA nanocapsules, the spectra show an intense C=O stretching mode associated with carbonyl of PMA at 1730 cm^{-1}.[14] The two observable peaks related to CHD

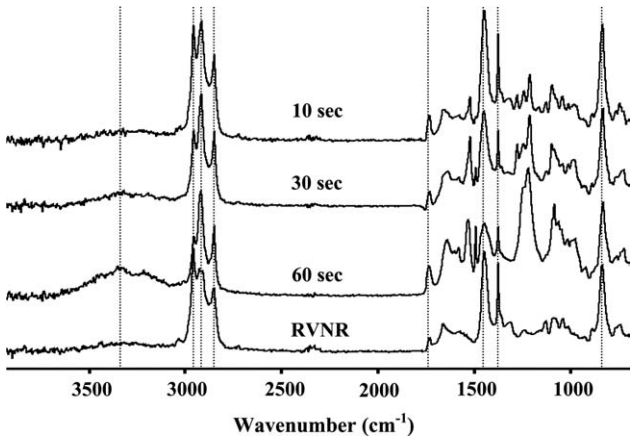

Figure 3 ATR-FTIR spectra of RVNR and CHD-PMA nanocapsules deposited onto the RVNR surface for various dipping times.

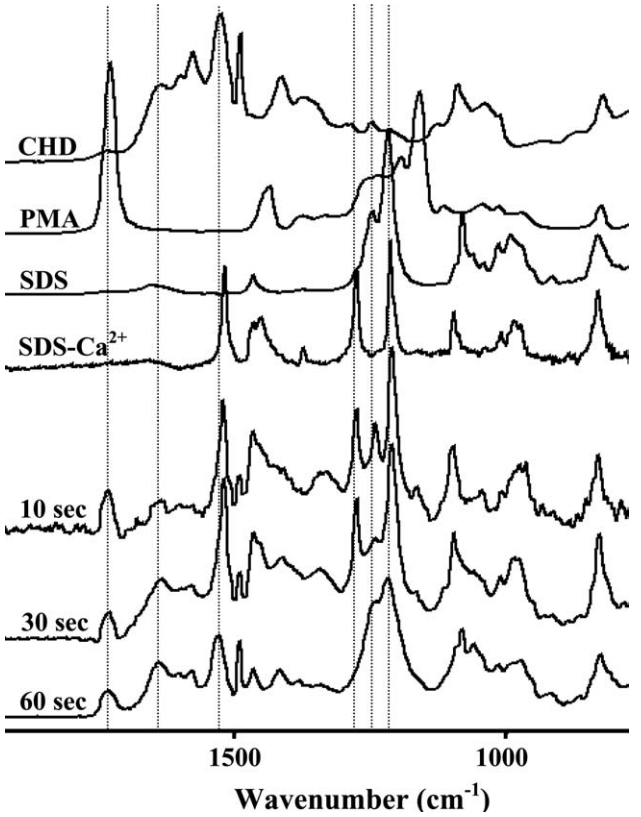

Figure 4 ATR-FTIR spectra of CHD, PMA, SDS on RVNR, SDS treated Ca^{2+} on RVNR, and CHD-PMA nanocapsules deposited on RVNR with different dipping times (10, 30, and 60 s) after subtraction of the RVNR spectrum.

appear in the spectrum of nanocapsules deposited onto RVNR sheet, i.e., (1) the broad band at 3450 cm^{-1}, possibly attributable to N—H stretching; and (2) an absorption peak at 1500–1650 cm^{-1} from C=C stretching of the aromatic moiety in the CHD molecule.[15,16] The result strongly supports that CHD-PMA nanocapsules are deposited onto the RVNR surface. However, the band characteristics of RVNR is still clearly observed in all samples with dipping times of 10, 30, and 60 s, indicating penetration of the infrared beam through the capsules layer to the RVNR base layer.

Complex vibrational modes in the region of 1600–1000 cm^{-1} are also observed in the spectra. To investigate the origin of these bands, the RVNR spectrum was subtracted from those of the capsule-coated samples to eliminate the rubber characteristics. These spectra are compared with those of PMA, CHD, SDS, and Ca^{2+}-treated SDS in Figure 4. All difference spectra show combinations of band characteristics of PMA at 1730 cm^{-1}, CHD at 1641 and 1530 cm^{-1}, and SDS at 1245 and 1214 cm^{-1} (asymmetric SO_2 stretching), respectively.[17] An increase in intensities of these vibrational modes as a function of dipping time indicates an increase in the degree of nanocapsules deposition.

Intriguingly, the spectra show changes in the vibrational modes of sulfate groups of SDS, i.e., two bands are observed at 1245 and 1214 cm^{-1} in the spectrum of the sample prepared using a dipping time of 60 s. This is similar to those found in the spectrum of the original SDS (neutralized by Ca^{2+}-cations). However, a new band is found at 1278 cm^{-1} in the spectra of the samples prepared using dipping times of 10 and 30 s. This band is probably due to sulfate groups bound with Ca^{2+}, as also observed in the spectrum of Ca^{2+}-treated SDS. The existence of this mode in the samples with dipping times of 10 and 30 s indicates the formation of electrostatic interaction between Ca^{2+} located at the RVNR surface and SDS molecules on the nanocapsules, which plays a key role in the initial stage of deposition. When the submersion time reaches 60 s, the band disappears, i.e., the interaction has diminished. This is because the nanocapsules are probably fused together and fully cover the RVNR surface, which prevents the formation of such interaction in the later stage of deposition. Nonetheless, the existence of the two lower frequency bands indicates the presence of SDS molecules in the nanocapsules layer.

The SEM micrographs of RVNR sheet and RVNR sheets covered with CHD-PMA nanocapsules as a function of dipping time are displayed in Figure 5.

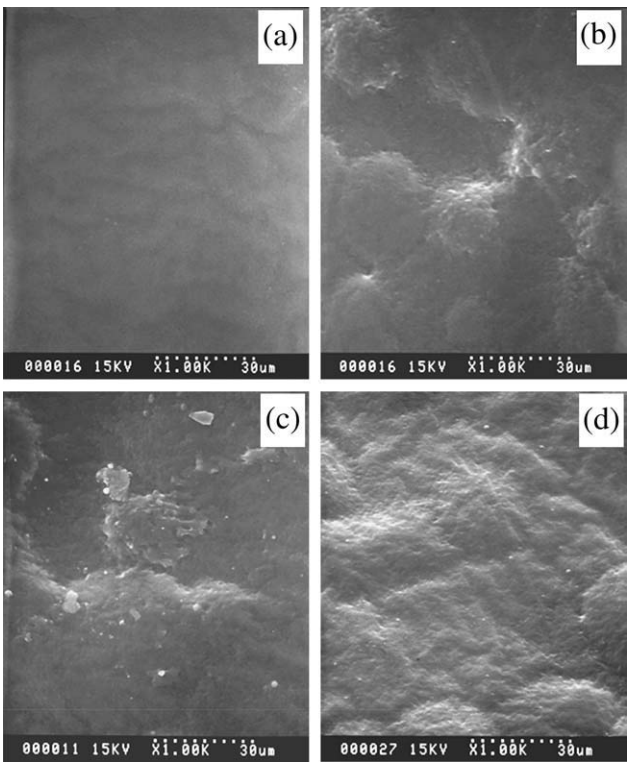

Figure 5 SEM micrographs of (a) RVNR sheet and RVNR sheets covered with CHD-PMA nanocapsules as a function of dipping time; (b) 30 s, (c) 5 min, and (d) 10 min.

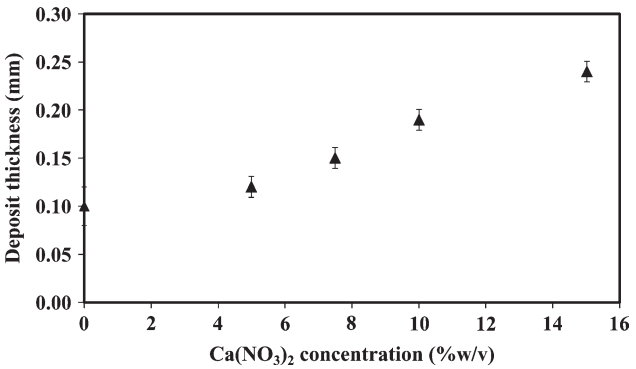

Figure 6 Effect of $Ca(NO_3)_2$ concentration on the thickness of RVNR/CHD-PMA nanocapsules (dipping time for 30 s)/RVNR three-layer film.

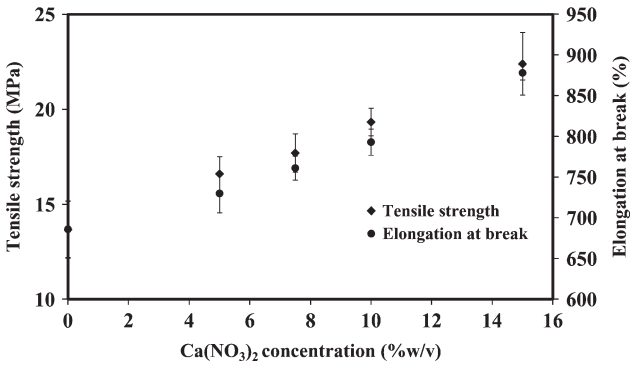

Figure 7 Effect of $Ca(NO_3)_2$ concentration on tensile strength and elongation at break of the RVNR/CHD-PMA nanocapsules/RVNR three-layer films.

A flat and smooth surface of the former is observed in Figure 5(a) when compared with the rough surface caused by the deposited CHD-PMA nanocapsules in the latter [Fig. 5(b–d)]. Because of the low glass transition temperature (T_g) of the PMA shell (15°C), the nanocapsules could fuse and form a film at room temperature.[18] From the micrographs, it can be deduced that the multilayer deposition took place by bridge formation of the nanocapsules to the rubber surface.[19]

Tensile properties and morphology of the three-layer film

Effect of coagulant concentration

The thickness of the RVNR/CHD-PMA nanocapsules/RVNR three-layer film obtained by using various concentrations of $Ca(NO_3)_2$ coagulant was measured and the data are presented in Figure 6.

The results show that the thickness of the RVNR/CHD-PMA capsules/RVNR three-layer film increased proportional to the $Ca(NO_3)_2$ concentration. This is because the higher amount of coagulant on the mold caused a higher rate of diffusion of the coagulant into the latex.[20,21] Without using coagulant, the three-layer film obtained was not uniform.

Because of the fact that some defects of the multilayer thin film might occur during the dipping process, the mechanical properties of the samples as a function of coagulant concentration were measured. The tensile strength and elongation at break of the three-layer films plotted versus $Ca(NO_3)_2$ concentrations are presented in Figure 7.

As observed in Figure 7 both tensile strength and elongation at break of the three-layer thin film linearly increase with increasing $Ca(NO_3)_2$ concentration. The high mechanical properties can be interpreted as the result of interparticle crosslinking through the Ca^{2+} and also of the high film thickness as presented in Figure 6.[22] On the other hand, the thin film obtained without using $Ca(NO_3)_2$ possessed low tensile strength and elongation at break, possibly due to defects, e.g., pinholes, generated during processing.[21]

Surface morphology

The SEM micrographs in Figure 8 show the surface morphologies of (a) the inner RVNR layer; (b) the

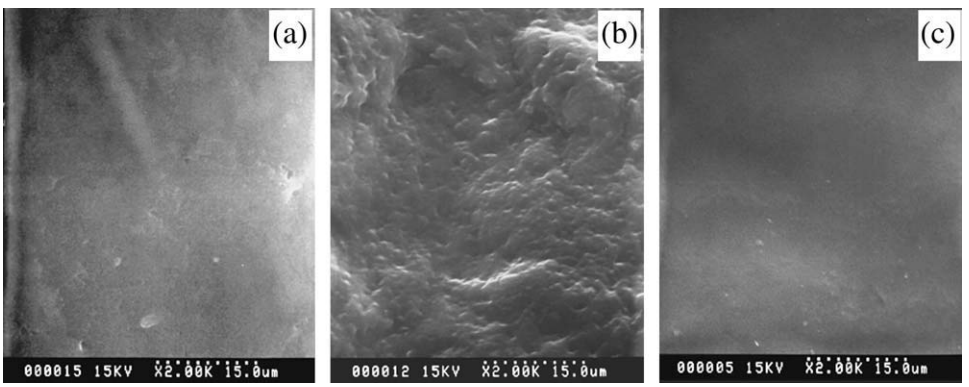

Figure 8 SEM micrographs of the surfaces of (a) inner RVNR layer; (b) RVNR film coat with CHD-PMA nanocapsules (dipping time = 30 s); and (c) the outermost RVNR layer.

RVNR film with CHD-PMA nanocapsules (dipping time = 30 s, using 5% $Ca(NO_3)_2$ as coagulant), and (c) the outermost RVNR layer.

It is observed in Figure 8(a) that the RVNR inner layer exhibits a rather smooth surface which might be attributed to slippage of the wet deposit formed on the mold. Figure 8(b) shows CHD-PMA nanocapsules deposited onto the inner RVNR layer. The multilayer of CHD-PMA nanocapsules covers the RVNR surface and the capsules are fused together due to the low T_g of the PMA shell. Finally, the outermost layer of RVNR was coated onto the nanocapsules middle layer, producing the three-layer thin film. The homogeneous and smooth surface morphology of the outer RVNR layer in Figure 8(c) confirms the advantage of multidipping where the pinholes running through the whole film, if at all existent, are absent. From the micrographs, it can be deduced that the RVNR/CHD-PMA nanocapsules/RVNR three-layer thin film has a suitable structure for further development of disinfectant medical glove's production due to the potential release of CHD for neutralization of infectious agents.

CONCLUSIONS

The size, shell thickness, and encapsulation efficiency of CHD-PMA nanocapsules were significantly improved when using a PMA shell with $\overline{M}_w$ of 550 K. The presence of nanocapsules on the RVNR latex sheet was deduced from the low contact angle value and ATR-FTIR spectra. Under SEM, multilayers of nanocapsules deposited onto the rubber with various dipping times were clearly observed. The coagulant dipping method was successfully used for preparation of the RVNR/CHD-PMA nanocapsules/RVNR three-layer thin film whose thickness and tensile properties increased with increasing concentration of coagulant. From SEM micrographs, it could be deduced that a three-layer structure was obtained, where the outermost and inner layers were RVNR and the active middle layer contained CHD-PMA nanocapsules. This structure was suitable for further development of disinfectant medical glove's preparation for the potential release of CHD for neutralization of the infectious agents carried by needles commonly used in medical practice.

References

1. Eklund, A. M.; Ojajärvi, J.; Laitinen, K.; Valtonen, M.; Werkkala, K. A. Ann Thorac Surg 2002, 74, 149.
2. Osman, M. O.; Jensen, S. L. World J Surg 1999, 23, 630.
3. Busnel, R. G.; Argy, G. U.S. Pat. 5,024,852 (1991).
4. Sonntag, P.; Hoerner, P.; Cheymol, A.; Argy, G.; Riess, G.; Rieter, G. Nat Mater 2004, 3, 311.
5. Bricout, F.; Moraillon, A.; Sonntag, P.; Hoerner, P.; Blackwelder, W.; Plotkin, S. J Med Virol 2003, 69, 538.
6. Paiphansiri, U.; Tangboriboonrat, P.; Landfester, K. Macromol Biosci 2006, 6, 33.
7. Paiphansiri, U.; Tangboriboonrat, P.; Landfester, K. Macromol Symp 2007, 251, 54.
8. Paiphansiri, U.; Tangboriboonrat, P. J Appl Polym Sci 2009, 112, 769.
9. Otsu, T. J Polym Sci Part A: Polym Chem 2000, 38, 2121.
10. Zhou, H.; Jiang, J.; Zhang, K. J Polym Sci Part A: Polym Chem 2005, 43, 2567.
11. Van Der Heiden, P. A.; Willems, M. G.; Lindhout, T.; Pijpers, A. P.; Koole, H. L. J Biomed Mater Res 1998, 40, 195.
12. Vinetsky, Y.; Magdassi, S. Colloid Polym Sci 1998, 276, 395.
13. Ratnam, T. C.; Nasir, M.; Baharin, A.; Zaman, K. Polym Int 2000, 49, 1693.
14. Chowdhury, P.; Pal, C. M. Eur Polym J 1999, 35, 2207.
15. Cortest'es, E. M.; Sinisterra, D. R.; Avilacampos, J. M.; Tortamano, N.; Rocha, G. R. J Inclsion Phenom Macrocycl Chem 2001, 40, 297.
16. Suci, A. P.; Geesey, G. G.; Bonnie, J. J Microbiol Methods 2001, 46, 193.
17. Socrates, G. Infrared Characteristic Group Frequencies: Tables and Charts; Wiley: New York, 1994.
18. Metin, B.; Blum, F. D. J Chem Phys 2006, 124, 054908.
19. Elimelechm, M. Particle Deposition and Aggregation: Measurement, Modeling and Simulation; Colloid and Surface Engineering Series; Butterworth-Heiemann: Woburn, MA, 1995.
20. Sasidharan, K. K.; Joseph, R.; Rajammal, G.; Pillai, V. P.; Gopalakrishnan, S. K. J Appl Polym Sci 2001, 81, 3141.
21. Blackley, D. C. Polymer Latices; Chapman & Hall: London, 1997.
22. Zin, W. WBM Radia Phys Chem 1998, 52, 611.